3D Reconstruction of Buildings from LiDAR Data

Marko Bizjak*

Supervised by: Domen Mongus†

Laboratory for Geometric Modelling and Multimedia Algorithms
University of Maribor Faculty of Electrical Engineering and Computer Science
Smetanova ulica 17, SI-2000 Maribor / Slovenia

Abstract

This paper presents a new approach to automatic 3D building reconstruction from LiDAR data. While traditional approaches use random sampling or Hugh transform for extracting subsets of coplanar points from noisy point clouds, our method is based on locally fitted surfaces (LoFS). These are planes, best-fitted to the K-neighbourhood of each LiDAR point. In this way, a set of candidate patches for a building surface is obtained. The clustering of patches is then performed based on the planes' normals and the positions of neighbourhoods, in order to obtain a rough approximation of flat roof sides. An adjacent graph is generated between them and intersections between neighbouring sides are estimated in order to define ridges, while intersections between buildings and ground points are considered in footprint definition. This defines the vertical walls. This method was tested on buildings of different architectural styles, sizes, and complexity. Most buildings are successfully reconstructed, however with increased building details, the accuracy of reconstruction is often decreased.

Keywords: LiDAR, Building, Reconstruction, LoFS

1 Introduction

Light Detection And Ranging (LiDAR) has become a popular research topic over the last decade, as more attention is directed towards Earth observations [10, 9]. LiDAR is an active remote sensing technology that utilises laser light in order to scan surface topographies, usually from an airborne platform. The result of such scanning is a dense cloud of topologically unstructured 3D points that allows accurate monitoring of the Earth's surface. Recently, 3D reconstruction of urban environment has become increasingly important and is being used for many applications such as urban planning [4], wireless communications' modelling [18], tourism or grand-scale virtual geographical information programs [19]. As manual reconstruction is exhausting, it is imperative to be able to reconstruct buildings automatically or semi-automatically.

This paper presents a novel method for automatic building reconstruction from LiDAR data that uses locally fitted surfaces (LoFS) in combination with clustering and an adjacency graph to find primary buildings' vertexes and borders. The paper is structured into 4 sections. The next section provides an overview of the related work. Section 3 describes the proposed method for reconstruction of buildings, followed by the results. The last section concludes this paper.

2 Related work

Automatic reconstruction of buildings from LiDAR data is an intensive research field, where a number of solutions have already been proposed. In most common cases, planar patches are extracted from point clouds in order to obtain approximated flat roof sides. Random sampling consensus (RANSAC) [2, 21, 22, 12, 1], Hugh transform [13, 20, 23], or region growing on surfaces [15, 7, 5, 17] are the most often used methods for this purpose.

An early attempt at semi-automatic reconstruction was done by Haala and Brenner [3]. In addition to LiDAR data they used 2D ground plans of buildings for their automatic 3D reconstruction. The ground plans are divided into rectangles, for each of which 3D primitives are instantiated. Final reconstruction is obtained by merging selected 3D primitives. Later, Brenner [2] presented a bottom-up approach that extracts faces from laser scan data using RANSAC. A set of rules was developed to decide which segments are selected for this purpose. The roof is then built from the selected segments, closing any gaps. Recently, Arikan et. al [1] introduced a reconstruction and modelling pipeline to create polygonal models from unstructured point clouds. They extracted planar patches using RANSAC and then snapped them together using an iterative optimisation approach.

In contrast, Vosselman [23] developed a method that uses Hough transform in order to extract planar faces from laser scan data, followed by a connected component analysis. The roof topology is determined by considering geometric constraints and bridging gaps along detected edges. Vosselman and Dijkman [24] upgraded this method by integrating the information obtained from ground plans.

---
*m.bizjak@um.si
†domen.mongus@um.si

In 2003, region growing on surfaces was utilised for reconstruction by Rottensteiner and Breise [17]. They proposed a method that uses LiDAR data in combination with aerial images. Roof planes are detected by a curvature-based segmentation technique [16]. They are grouped to create polyhedral building models and then improved with the usage of all available sensor information. A region growing algorithm based on an adjacency graph was proposed by Milde et al. [7]. Simple roof shapes are extracted by finding subgraphs, whereas complex roof structures are derived using formal grammar.

The idea of presenting topological relations between approximated roof sides using adjacency graph was first introduced by Verma et al. [22], where two faces are considered as adjacent if at least one pair of line segments from their approximated 3D boundaries is close enough. Several other approaches have also been proposed for establishing adjacency relations. Milde et al. [7] used the perpendicular distance between oriented parallel bounding boxes of faces. Oude Elberink [14] considered the length of a segment, determined by points within a flexible distance from intersection lines between two faces.

3 Reconstruction of buildings

Reconstruciton is performed over four steps. Firstly, locally fitted surfaces (LoFS) are estimated for each point. In the next step DBSCAN clustering is applied on the normals and position of the neighbourhood in order to obtain approximated flat roof sides. An adjacency graph is constructed in the third step and in the last step main buildings' borders and sides are estimated. Every step is separately described in detail in the following subsection.

3.1 Estimation of LoFS

The method's input is a LiDAR point cloud, where each point is georeferenced and classified as building, terrain or vegetation [8]. Firstly, for each building point, the K-nearest points are located using fast approximate K-nearest neighbours algorithm [11]. A plane is fitted to the K-neighbourhood of each point using locally fitted surfaces (LoFS). LoFS is a set of best-fitted surfaces to the K-neighbourhood of each point [8]. If the neighbourhood of each point does not belong to the same surface, large-fitting error occurs. In this case, a surface with better-fit should exist. In order to determine it, the neighbourhood of each point is inspected. For better understanding, consider the example in Figure 1a), where a case of six points from a roof surface and a point within the building is presented. Firstly, a set of best-fitting surfaces is estimated in Figure 1b) with a fitting window size set to 3 and linking window size to 5. Window size defines the number of points considered when fitting or linking surfaces. In our case this means that each surface is fitted to a given point by also considering its neighbour on each side. Ev-
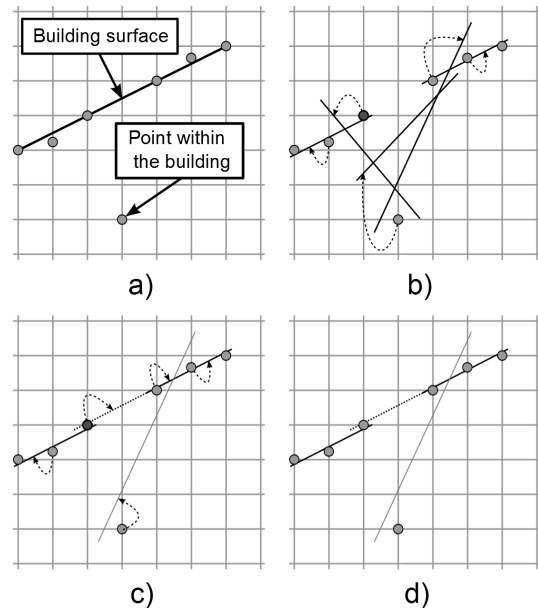

Figure 1: Estimation of LoFS with window size for fitting set at 3 and for linking at 5 in the case of a noisy surface a). A set of best-fitted surfaces is obtained and linked with the corresponding points b). The neighbourhood of each point is inspected to link it with a surface with the best fit c) in order to obtain the final set of surfaces d).

ery point is linked to the fitted surface, as shown in Figure 1b). During the linking step, the neighbourhood of 2 points on each side of the given point are inspected for the defined window size. The surface from this neighbourhood with the lowest distance (error) to a given point is linked with it. Thus, the darkened point is linked with the surface corresponding to the second neighbour on its right (as shown in Figure 1c)). The final set of surfaces can be seen in Figure 1d).

3.2 Clustering

Points linked with their LoFS are then clustered separately by normals and then by position in order to obtain a rough approximation of flat roof sides. Clustering is a process of dividing data into groups of similar objects (clusters). Density based spatial clustering (DBSCAN) within large datasets with noise is used [6], as LiDAR point cloud is a representative of such datasets. DBSCAN is based on the idea that the density within a neighbourhood for an object has to be high enough to belong to a cluster. Each cluster is created from a single data object by absorbing all objects in its neighbourhood. DBSCAN is independent of data order. It is controlled by two parameters: the minimal number of points required to be considered as a cluster and density treshold for neighbourhoods. In this step clusters of points that belong to the same flat roof side are obtained. The problem of using density within a neighbourhood for clustering is that DBSCAN also clusters points within the

neighbourhood that might be a part of a curved surface. This only occurs when the curvature is small enough for the distance between neighbours to be lower than the density threshold. Each cluster with an averaged plane equation is considered as a node of the adjacency graph that is constructed in the next step. The result of such clustering is presented in Figure 2.

Figure 2: Example of clusters of points that belong to the same flat roof side (i. e. nodes) for a building's roof.

3.3 Adjacency graph construction

The topological relations between approximated roof sides are usually presented in an adjacency graph. Adjacency is commonly defined as a pair-wise connection by an edge between two roof sides that share a common border [22]. In order to be able to detect common ridge points, we define adjacency as edges between roof sides that share at least one ridge point. Adjacency is tested using enlarged and oriented bounding boxes of the approximated roof sides. If two bounding boxes overlap, they are adjacent. In this way an undirected graph is constructed, as shown in Figure 3.
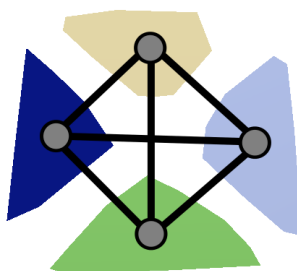

Figure 3: Adjacency graph for a roof with four nodes that share the same ridge point. Black segments represent graph edges.

3.4 Modelling

In order to reconstruct a building we need to determine its boundary points and edges. Firstly, ridge points that are shared between at least three roof sides are estimated. This

is performed by searching for maximal cliques in the adjacency graph. Clique is a subset of nodes in an undirected graph where every two nodes in the subset are connected by an edge. It is maximal when it does not exist within a larger clique. From every clique we select three nodes that share at least one border with the other two nodes. To test if two nodes share a common border, an intersection line between pairs of nodes is first calculated. Then the points of each node that are within a certain distance d from the intersection line are projected perpendicularly on the line, as shown in Figure 4.
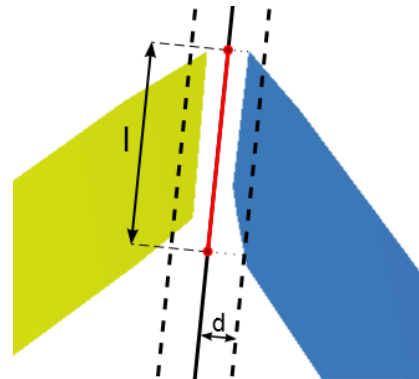

Figure 4: Shared common border between a pair of nodes. Points within a distance d from both nodes are perpendicularly projected on the intersection line. The longest segment between projected points l needs to be long enough.

If the longest segment l between the projected points from both nodes is long enough (e.g. 1m), it is considered that there is a border between these nodes. Using the selected three nodes we calculate a shared ridge point as the intersection point of three planes. The calculated ridge point is shared amongst all nodes in the clique. After we have obtained ridge points, the borders between nodes are estimated. A border is a segment on an intersection line between two nodes. A segment is bounded by either a ridge point or the projection of a bounding point of a node. There are two types of bounding points of a node used for projection.
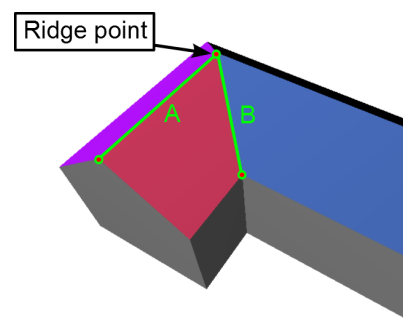

Figure 5: Border bounding points determination based on the type of a border (A - horizontal, B - inclined).

Suppose we have a building designed as shown in Figure 5, we already know the marked ridge point and we need to determine borders A and B. If an intersection line is horizontal (A), it represents a ridge, thus the bounding point of a border is the perpendicular projection of a node point to the intersection line in such a way that the border is maximally long. If it is not horizontal (B), then the bounding point of a border is the point on the intersection line with the same height as for the lowest point from both intersecting nodes. After the bounding points and borders of a roof are determined, we need to determine the building's exterior walls' height. This height is obtained from LiDAR data as the difference to the lowest ground point in direct proximity to the building.

4 Results

The presented method was tested on LiDAR datasets with a wide variety of building types. The tested buildings were of different sizes, architecture and complexity. We were limited by LiDAR data sparsity as the number of points on each planar surface needs to be large enough for successful extraction of flat roof sides. Consequently, only those flat roof sides that are large enough were successfully extracted and used during the process of reconstruction.

During the first step we fitted to the neighourhood of 8 points (K=8). The fitting and linking window sizes were also set to 8. At least 5 points were needed to form a cluster in the next step. When clustering by position and normals were performed, densities of 1.4 and 0.12 were used, respectively. In the third step for the adjacency test the oriented bounding boxes were enlarged by 1m in all directions. For the shared common border test d and the minimum length of l were both set to 1m. All the presented results were tested using these settings. The result of the reconstruction of a single building without complex parts is presented in Figure 6.
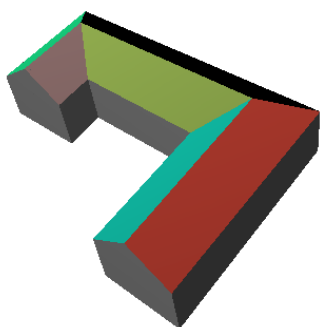

Figure 6: Reconstruction of a building with large surfaces.

Common ridge points and borders were successfully determined. Additionally we are able to reconstruct more complex buildings with smaller roof surfaces, as shown in

Figures 7 and 8. For better comparison, LiDAR datasets for these two reconstructed buildings are shown in Figures 7a) and 8a), where the building points are red and ground points brown. The capabilities of reconstruction include a hipped roof and embedding gable to the larger roof sides, as can be seen in Figure 7.
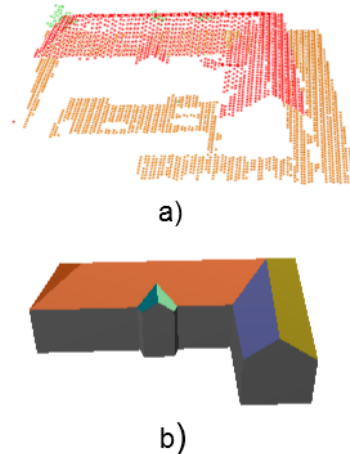

a)

b)

Figure 7: Reconstruction of a building b) with embedded gable and hipped roof on the left side from LiDAR data a).

Figure 8 presents an example of a reconstruction that incorporates shed dormer into the building. Dormers can be located anywhere on the larger roof surface as long as the first two steps have successfully extracted its planar surfaces. In addition we performed testing on larger Li-
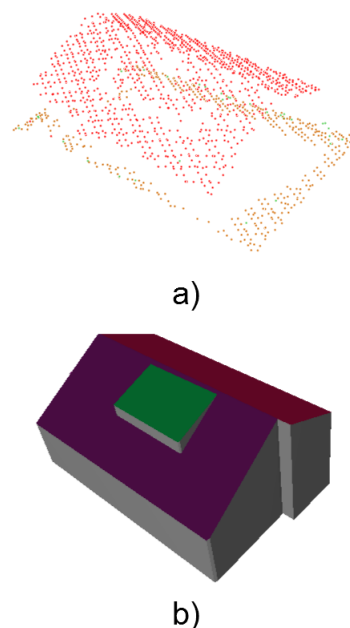

a)

b)

Figure 8: Reconstruction of a building b) with embedded shed dormer from LiDAR data a).

DAR datasets. As can be seen in Figures 9 and 10, this method provides good reconstruction of buildings from LiDAR datasets with a greater number of buildings.
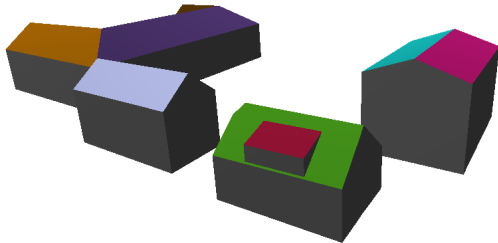

Figure 9: Example of successfully reconstructed buildings of a small settlement from LiDAR dataset.
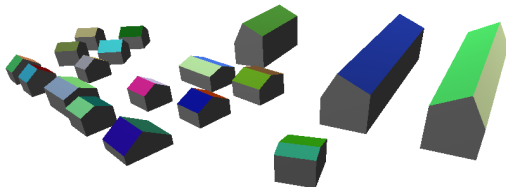

Figure 10: Reconstruction of a settlement.

5 Conclusions

This paper proposed a novel method for the reconstruction of buildings from LiDAR data. For the extraction of approximated roofs' planar faces the locally fitted surfaces (LoFS) and DBSCAN clustering were used. Between the obtained planar faces an adjacency graph was constructed for extracting the common ridge points. The borders between the faces and building's exterior walls were estimated for the final building model. To our knowledge this is the first method using this concept of LoFS for the estimation of planar surfaces. The results confirmed that the method can successfully reconstruct most regularly complex buildings with sufficient accuracy.

There are many possibilities for the improvement of reconstruction during all steps. Different clustering algorithm could provide better planar faces extraction results as DBSCAN clusters points within the neighbourhood that might also be a part of a curved surface. For faster computation a subgraph of the adjacency graph from the third step, that would define adjacency more strictly, could be used for border estimation. Modelling improvements are possible on many levels such as multi-layered building roofs, curved roofs or facade design.

References

[1] M. Arikan, M. Schwärzler, S. Flöry, M. Wimmer, and S. Maierhofer. O-snap: Optimization-based snapping for modeling architecture. *ACM Trans. Graph.*, 32(1):1–15, 2013.

[2] C. Brenner. Towards fully automatic generation of city models. *International Archives of Photogrammetry and Remote Sensing*, 33(B3/1):84–92, 2000.

[3] C. Brenner and N. Haala. Rapid acquisition of virtual reality city models from multiple data sources. *International Archives of Photogrammetry and Remote Sensing*, 32:323–330, 1998.

[4] J. Döllner, T. H. Kolbe, F. Liecke, T. Sgouros, and K. Teichmann. The virtual 3D city model of Berlin-managing, integrating, and communicating complex urban information. In *Proceedings of the 25th Urban Data Management Symposium UDMS*, 2006.

[5] P. Dorninger and N. Pfeifer. A comprehensive automated 3D approach for building extraction, reconstruction, and regularization from airborne laser scanning point clouds. *Sensors*, 8(11):7323–7343, 2008.

[6] M. Ester, H. Kriegel, J. Sander, and X. Xu. A density-based algorithm for discovering clusters in large spatial databases with noise. *KDD*, 96(34):226–231, 1996.

[7] J. Milde, Y. Zhang, C. Brenner, L. Plmer, and M. Sester. Building reconstruction using a structural description based on a formal grammar. *The International Archives of the Photogrammetry, Remote Sensing and Spatial Information Sciences*, 37:227–232, 2008.

[8] D. Mongus, N. Lukač, and B. Žalik. Ground and building extraction from LiDAR data based on differential morphological profiles and locally fitted surfaces. *ISPRS Journal of Photogrammetry and Remote Sensing*, 93:145 – 156, 2014.

[9] D. Mongus and B. Žalik. Parameter-free ground filtering of LiDAR data for automatic DTM generation. *ISPRS Journal of Photogrammetry and Remote Sensing*, 67:1–12, 2012.

[10] D. Mongus and B. Žalik. Computationally efficient method for the generation of a digital terrain model from airborne LiDAR data using connected operators. *IEEE Journal of Selected Topics in Applied Earth Observations and Remote Sensing*, 7(1):340–351, 2014.

[11] M. Muja and D.G. Lowe. Scalable nearest neighbor algorithms for high dimensional data. *IEEE Transactions on Pattern Analysis and Machine Intelligence*, 36(11):2227–2240, 2014.

[12] L. Nan, A. Sharf, H. Zhang, D. Cohen-Or, and B. Chen. Smartboxes for interactive urban reconstruction. *ACM Trans. Graph.*, 29(4):1–10, 2010.

[13] A. Novacheva. Building roof reconstruction from Li-DAR data and aerial images through plane extraction and colour edge detection. *The International Archives of the Photogrammetry, Remote Sensing and Spatial Information Sciences*, 37:53–57, 2008.

[14] S. Oude Elberink. Target graph matching for building reconstruction. *International Archives of Photogrammetry, Remote Sensing and Spatial Information Sciences*, 38:49–54, 2009.

[15] J. Park, I. Lee, Y. Choi, and J. Y. Lee. Automatic extraction of large complex buildings using LiDAR data and digital maps. *International Archives of Photogrammetry and Remote Sensing*, 36:148–154, 2006.

[16] F. Rottensteiner and C. Briese. A new method for building extraction in urban areas from high-resolution LiDAR data. *International Archives of Photogrammetry Remote Sensing and Spatial Information Sciences*, 34(3/A):295–301, 2002.

[17] F. Rottensteiner and C. Briese. Automatic generation of building models from LiDAR data and the integration of aerial images. *Int. Arch. of Photogrammetry and Remote Sensing*, 34:174–180, 2003.

[18] T.K. Sarkar, Zhong Ji, Kyungjung Kim, A. Medouri, and M. Salazar-Palma. A survey of various propagation models for mobile communication. *Antennas and Propagation Magazine, IEEE*, 45(3):51–82, 2003.

[19] S. Sheppard and P. Cizek. The ethics of Google Earth: Crossing thresholds from spatial data to landscape visualisation. *Journal of Environmental Management*, 90(6):2102 – 2117, 2009.

[20] G. Sohn, X. Huang, and V. Tao. Using a binary space partitioning tree for reconstructing polyhedral building models from airborne LiDAR data. *Photogrammetric Engineeering and Remote Sensing*, 2008.

[21] F. Tarsha-Kurdi, T. Landes, and P. Grussenmeyer. Extended RANSAC algorithm for automatic detection of building roof planes from LiDAR data. *The photogrammetric journal of Finland*, 21(1):97–109, 2008.

[22] V. Verma, Rakesh Kumar, and S. Hsu. 3D building detection and modeling from aerial LiDAR data. 2:2213–2220, 2006.

[23] G. Vosselman. Building reconstruction using planar faces in very high density height data. *IAPRS*, 32(3):87–92, 1999.

[24] G. Vosselman and S. Dijkman. 3D building model reconstruction from point clouds and ground plans. 34(3/W4):37–44, 2001.